Thermoelectric cooling materials

3 authors:

Jun Mao
Harbin Institue of Technology Shenzhen
83 PUBLICATIONS   3,884 CITATIONS

Gang Chen
Guangdong Ocean University
741 PUBLICATIONS   55,117 CITATIONS

Zhifeng Ren
Boston College, USA
540 PUBLICATIONS   34,604 CITATIONS

Some of the authors of this publication are also working on these related projects:

Project   Thermoelectric Materials: Experiments and Simulations   View project

Project   Mg2Sn based solid solutions   View project

Thermoelectric cooling materials

Jun Mao[1], Gang Chen [2] and Zhifeng Ren [1]✉

Solid-state thermoelectric devices can directly convert electricity into cooling or enable heat pumping through the Peltier effect. The commercialization of thermoelectric cooling technology has been built on the Bi$_2$Te$_3$ alloys, which have had no rival for the past six decades around room temperature. With the discovery and development of more promising materials, it is possible to reshape thermoelectric cooling technology. Here we review the current status of, and future outlook for, thermoelectric cooling materials.

n 1834, Jean Peltier discovered that there is a heating or cooling effect when electric current flows through the junction of two dissimilar metals[1]. The principle of the Peltier effect is that when current flows across an interface, heat is absorbed (cooling) or rejected (heating) owing to the difference in the thermal energy transported by charge carriers (electrons or holes) in the two materials. Using the Peltier effect as a means of refrigeration was first seriously considered in 1911 by Altenkirch[2]. Early attempts to devise thermoelectric coolers, however, were unsuccessful because of the lack of high-performance materials[3]. It was not until the 1950s that an appreciable Peltier cooling effect was realized in semiconductors[4–6]. Subsequently, there was an explosion of interest in thermoelectric cooling, as it was expected to be as efficient as vapour compression cooling once the materials were improved. However, it was soon realized that such refrigerators could not compete against the existing mechanical refrigerators in terms of price and efficiency. Consequently, most of the work on thermoelectric cooling stopped in the mid-1960s[7]. Interest re-emerged in the 1990s with the awareness of the environmental impact of the fluids used for vapour compression refrigeration[8]. Today, thermoelectric coolers are used in specific applications (see Box 1), and the market for thermoelectric modules is growing.

In the past two decades, however, the vast majority of research has focused on materials that are promising for power generation at medium and high temperatures, and there have been few reports on cooling below room temperature. Whereas the commercialization of thermoelectric cooling has been realized for several decades, thermoelectric power generation is still in its infancy. Thermoelectric modules for power generation demand high thermal stability of the materials at elevated temperatures, minimum diffusion of the elements under an extreme temperature gradient (several hundred kelvin across a couple of millimetres), and an excellent match of the coefficients of thermal expansion between the n- and p-type legs for minimum thermal stress, in addition to high thermoelectric performance. In contrast, thermoelectric coolers are often used near ambient temperature, and the temperature difference between the hot and cold sides is usually less than 100 K. Thermal stability, thermal stress and the diffusion of elements are thus not severe issues, and the engineering and manufacturing processes for thermoelectric cooling modules are well established. With the discovery of high-performance materials, it is possible to advance thermoelectric cooling technology.

In this Perspective, concepts underlying the thermoelectric cooling performance will be introduced first. Subsequently, we will summarize state-of-the-art materials and discuss Bi$_{1-x}$Sb$_x$, Bi$_2$Te$_3$ alloys and Mg$_3$Bi$_{2-x}$Sb$_x$ in detail. Additionally, we will discuss ideas for identifying promising materials. We conclude with a discussion of the outlook and challenges of thermoelectric cooling materials and technology. As this Perspective is not intended to be comprehensive, readers interested in additional details are directed to other reports[9–11].

Cooling performance

Coefficient of performance. The cooling power (Q_C) for a thermoelectric unicouple consisting of an n-type leg and a p-type leg is[12]

$$Q_C = (S_p - S_n)IT_C - \frac{1}{2}I^2R - K(T_H - T_C) \tag{1}$$

where I is the electrical current; T_H and T_C are the hot- and cold-side temperatures, respectively; S_p and S_n are the respective Seebeck coefficients for the p-type and n-type thermoelectric legs; and R and K are the total electrical resistance and thermal conductance of the unicouple, respectively. To maximize the cooling power, the unicouple is expected to have a large ($S_p - S_n$) and small R and K values. As a result, the thermoelectric performance of an ideal unicouple can be measured by the figure of merit Z, where $Z = (S_p - S_n)^2 R^{-1} K^{-1}$.

The voltage of the external power source applied to the unicouple should be equal to the sum of the voltage drop due to the electrical resistance and the Seebeck voltage induced by the temperature difference. Therefore, the input electrical power (P) for a unicouple is[13]

$$P = I\big[RI + (S_p - S_n)(T_H - T_C)\big] \tag{2}$$

The cooling efficiency of a unicouple is quantified by the amount of cooling divided by the electrical power input. This efficiency is known as the coefficient of performance (COP). Since the cooling power and the input power are both functions of electrical current, COP can be maximized at an optimal electrical current. The maximum COP at given T_H and T_C values is[6,12]

$$COP = \frac{Q_C}{P} = \frac{T_C}{T_H - T_C} \frac{\sqrt{1 + ZT_m} - \frac{T_H}{T_C}}{\sqrt{1 + ZT_m} + 1} \tag{3}$$

where ZT_m is the averaged ZT between T_H and T_C. The COP, which is dependent on temperature difference ($\Delta T = T_H - T_C$), is calculated (the solid lines) and shown in Fig. 1a. The symbols represent the experimental COP values of thermoelectric cooling systems

[1]Department of Physics and Texas Center for Superconductivity at the University of Houston, University of Houston, Houston, TX, USA. [2]Department of Mechanical Engineering, Massachusetts Institute of Technology, Cambridge, MA, USA. ✉e-mail: zren@uh.edu

Box 1 | Thermoelectric cooling applications

Refrigerants, as used in the vapour compression cycles, can deplete the ozone layer and are extremely potent greenhouse gases. In contrast, solid-state thermoelectric coolers are much more environmentally friendly. Thermoelectric cooling devices have the advantages of being reliable, compact in size, silent in operation, relatively lightweight, capable of providing rapid heating and cooling, and able to realize precise control of temperature. Additionally, a thermoelectric system has much more flexible cooling power, which can be easily tuned by electrical current, than a system using vapour compression refrigeration[8]. A high COP can be achieved for a vapour compression refrigerator only when its cooling capacity is rather large[13]; in practice, the COP is reduced with the lowering of cooling capacity, in contrast to the thermoelectric cooler, which has a COP that is more or less independent of its cooling capacity[66].

Small-scale cooling. Generally, conventional vapour compression refrigeration systems are not competitive, in terms of cost and efficiency, with thermoelectric cooling when the heat load is under 25 W (ref. [67]). Currently, thermoelectric coolers have been mainly used in applications that require a small cooling power[12,66], such as portable refrigerators for carrying medical supplies[68] and for food storage[69]; cooling laser diodes and infrared, X-ray and gamma-ray detectors[70]; thermal cyclers for DNA synthesizers[71]; and temperature control of car seats[72].

Large-scale cooling. In large systems, in which the electrical power consumption is an essential consideration due to the cost of power, the COP of the cooling technology is critical[73]. Because of the low COP of the thermoelectric cooling system (Fig. 1a), it is challenging for it to be economically viable for large-scale cooling applications. Nevertheless, large thermoelectric cooling systems with high cooling power have been developed for specific applications, such as air conditioning for large buildings, railway coaches and submarines[74]. The use of large thermoelectric cooling systems has proved their technical reliability, but not their economic feasibility.

Hot-spot cooling. A refrigerator is normally used to maintain a heat source at a temperature below that of its surroundings. When the heat source must be prevented from rising above a temperature that is greater than ambient, a heat sink is usually employed rather than a refrigerator[13]. Passive cooling is often realized by heat spreading using materials with high thermal conductivity. A copper heat spreader, for example, can remove heat equalling $\kappa_{Cu} A \Delta T / L$, where κ_{Cu} is the thermal conductivity of copper and A and L are the cross-section and thickness of the copper plate, respectively. Thermoelectric cooling has been considered as a potential thermal management solution for electronics[75]. The maximum heat extraction by a thermoelectric cooler (neglecting the heat removed by thermal conduction down the thermoelectric elements) is[76]

$$Q = \frac{A T_H^2}{2L} \frac{\left(S_P - S_n\right)^2}{\left(\sqrt{\rho_P} + \sqrt{\rho_n}\right)^2}$$ (5)

and the thermoelectric elements are assumed to have the same dimensions as the copper plate. If the thermoelectric device is to remove more heat than a copper plate, the following conditions should be satisfied:

$$\frac{T_H^2}{2} \frac{\left(S_P - S_n\right)^2}{\left(\sqrt{\rho_P} + \sqrt{\rho_n}\right)^2} > \kappa_{Cu} \Delta T$$ (6)

Given the currently available materials, the thermoelectric device would perform better than the copper plate only when $\Delta T < 2$ at the T_H of 300 K (refs. [76,77]). Furthermore, owing to Joule heating of the thermoelectric legs, more heat is added to the hot side that must be carried to the environment. In fact, for hot-spot thermal management of electronics by lateral heat spreading, one should look for materials with not only a large power factor but also a high thermal conductivity[78], which is different from the traditional high-zT materials.

(red symbols) and vapour compression refrigerators and air conditioners (blue symbols). At a given temperature difference, COP increases with a higher ZT_m. Therefore, improving the performance of the unicouple is crucial for promoting the efficiency of a thermoelectric cooler. It should be noted, however, that the actual COP values for the system are lower than the prediction based on $ZT_m = 0.5$, although the thermoelectric elements have higher measured ZT_m. This discrepancy is mainly attributed to parasitic losses such as thermal resistances between the thermoelectric module and fluids and other heat leakages within the module. Compared with refrigerators and air conditioners based on the vapour compression cycle, thermoelectric cooling systems exhibit much lower COP values[14–17]. To achieve energy efficiencies that compete with those of conventional refrigerators, an extraordinary leap in the performance of materials is required ($ZT_m \approx 4$). Discouragingly, it is difficult to see how such a high ZT_m could be realized in the foreseeable future. As a result, thermoelectric cooling should be regarded not as a competitor to the conventional methods, but rather as a complementary technique for specialized applications[12].

Maximum temperature difference

In addition to COP, the capability to achieve a low temperature at the cold side for a given hot-side temperature (that is, the temperature difference) also quantifies the cooling performance of a unicouple.

A maximum temperature difference (ΔT_{max}) between the hot and cold sides depends on the ZT, and it can be expressed as[6,12]

$$\Delta T_{max} = \frac{1}{2} Z T_C^2$$ (4)

The ZT_m-dependent ΔT_{max} of a unicouple is calculated and shown in Fig. 1b, where the ΔT_{max} increases monotonically with ZT_m. The ZT_m is ~0.7 for a unicouple of the commercial Bi_2Te_3 alloys, and it corresponds to a ΔT_{max} of ~70 K at the hot-side temperature of 300 K. The hot-side-temperature-dependent ΔT_{max} for a single-stage cooler using Bi_2Te_3 alloys is calculated and shown in Fig. 1c. Since the ΔT_{max} is reduced with decreasing hot-side temperature, thermoelectric coolers become inefficient in the low-temperature range ($T_H < 150$ K, the grey shaded area). Even with 50% enhancement in ZT_m of both n-type and p-type Bi_2Te_3 alloys, which would be a formidable challenge, the improvement in ΔT_{max} is still insignificant in the low-temperature range. It should be noted that the ΔT_{max} is achievable only at zero cooling power. In other words, for a given thermal load, which requires a finite cooling power, the temperature difference will be smaller than ΔT_{max} (ref. [18]). Although thermoelectric cooling at very low temperatures (in the liquid helium range or less) has been considered[13,19], the idea remains to be validated experimentally. In practice, most thermoelectric cooling
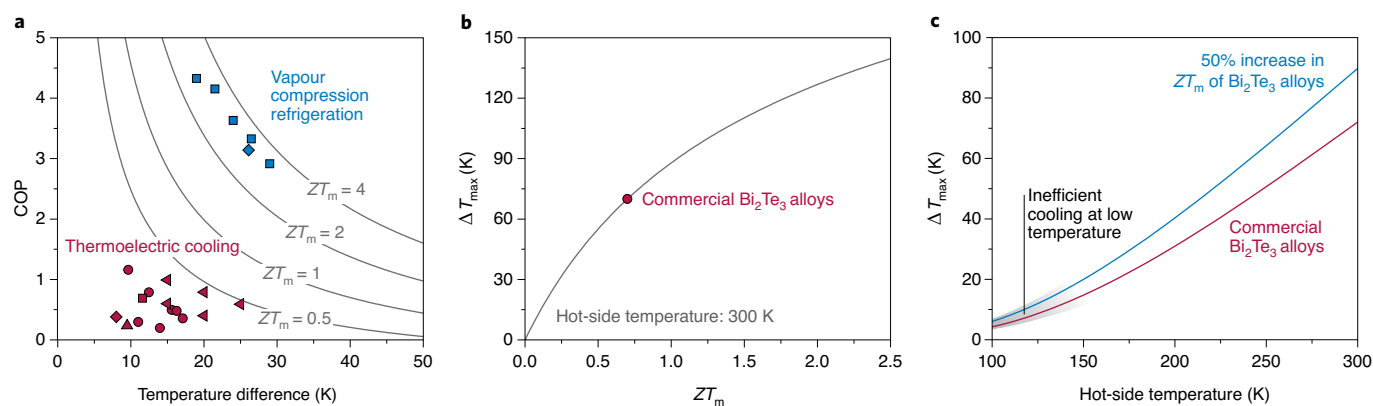
Fig. 1 | Thermoelectric cooling performance. a, A comparison of the COP values between thermoelectric cooling systems[15–17,60,61] and vapour compression refrigerators and air conditioners[62,63]. The solid lines are calculated by assuming that the hot-side temperature is 300 K, and the filled symbols are experimental values. The COP is calculated using constant ZT_m values, which implicitly assume that the thermoelectric transport properties are independent of temperature. **b**, Relationship between the ZT_m of the unicouple and the maximum temperature difference at the hot-side temperature of 300 K. **c**, Relationship between the maximum temperature difference and the hot-side temperature for the unicouple based on the state-of-the-art Bi_2Te_3 alloys. The measured temperature-dependent thermoelectric properties of commercial Bi_2Te_3 alloys are used for this calculation. The blue line shows the theoretical ΔT_{max} for those alloys given a 50% increase in ZT_m.

applications are close to room temperature, except for specific electronic cooling applications that achieve the required low temperatures by using multistage coolers (see Box 2).

State-of-the-art materials

The thermoelectric performance of a single n-type or p-type material is measured by $zT = S^2\rho^{-1}\kappa^{-1}T$, where ρ is the electrical resistivity and κ is the thermal conductivity. Although many materials with zT above unity at medium and high temperatures have been discovered over the past two decades, progress in developing materials for thermoelectric cooling has been unsatisfactory. The state-of-the-art low-temperature and room-temperature thermoelectric materials, including n-type $YbAl_3$ (ref. [20]), $Cu_{0.9}Ni_{0.1}AgSe$ (ref. [21]), $Bi_2Te_{3-x}Se_x$ (ref. [22]), $Mg_3Bi_{1.25}Sb_{0.75}$ (ref. [23]) and $Bi_{0.905}Sb_{0.095}$ (ref. [24]), and p-type $Bi_{2-x}Sb_xTe_3$ (ref. [22]), $CePd_{2.95}$ (ref. [20]), $Ce(Ni_{0.6}Cu_{0.4})_2Al_3$ (ref. [25]) and $CsBi_4Te_6$ (ref. [26]), are summarized in Figs. 2a and 2b, respectively. A further comparison of the figure of merit z, as the materials' intrinsic property, among several high-performance materials is shown in Fig. 2c. As can be seen, only Bi_2Te_3 alloys, $CsBi_4Te_6$ and $Mg_3Bi_{2-x}Sb_x$ exhibit high performance near room temperature, and only $Bi_{1-x}Sb_x$ excels below 150 K. There is an obvious reason that realizing high zT at low temperature is difficult: the low T. Thus, there is a challenging requirement for a very high z, which requires a highly favourable combination of several fundamentally contradictory attributes in the same material. Thermoelectric cooling performance has thus far been mainly reported for $Bi_{1-x}Sb_x$, Bi_2Te_3 alloys and $Mg_3Bi_{2-x}Sb_x$, and the following discussion will be limited to these materials.

$Bi_{1-x}Sb_x$. Bismuth and antimony are semimetals with small band overlap energies (the overlap energy of the conduction and valence bands). Bismuth has a low density-of-states effective mass ($m^\star$) of ~$0.1m_0$ (where m_0 is the free electron mass) for the conduction band[27], thus leading to an exceptionally high room-temperature electron mobility (μ) of the order of 10^4 cm^2 V^{-1} s^{-1} along the preferred orientation[13]. As a result, single-crystalline bismuth exhibits the highest weighted mobility, $\mu(m^\star/m_0)^{3/2}$, of any known thermoelectric material[13]. Semimetals usually have a low Seebeck coefficient due to the simultaneous presence of electrons and holes, but bismuth has a large negative Seebeck coefficient due to its large electron-to-hole weighted mobility ratio[27], $(\mu_e/\mu_h)(m_e^\star/m_h^\star)^{3/2}$, where subscripts e and h represent electrons and holes, respectively

(Fig. 2d). Polycrystalline bismuth exhibits a room-temperature Seebeck coefficient of about −70 μV K^{-1}, and for single-crystalline bismuth it is about −100 μV K^{-1} along the trigonal axis[27] (Fig. 2e). Such favourable electronic properties give rise to large power factor ($S^2\rho^{-1}$) values of ~77 μW cm^{-1} K^{-2} at 300 K and ~200 μW cm^{-1} K^{-2} at 100 K in single-crystalline bismuth[27].

Substitution of bismuth by antimony can greatly alter the band structure of bismuth, and $Bi_{1-x}Sb_x$ compositions with 0.07 < x < 0.22 are semiconductors with a small bandgap that exhibits a maximum at around 15–17 at% antimony[24]. The semiconducting $Bi_{1-x}Sb_x$ shows a large Seebeck coefficient and a substantially reduced thermal conductivity, and thus its thermoelectric performance is effectively improved[24,28]. Single-crystalline $Bi_{1-x}Sb_x$ exhibits the highest z among all of the reported materials below 150 K (Fig. 2c), and it is promising for low-temperature thermoelectric cooling. Further substantial enhancement in the thermoelectric performance of $Bi_{1-x}Sb_x$ can be achieved by applying a transverse magnetic field (with a peak z of 8.6×10^{-3} K^{-1} at 100 K)[29], benefiting from the thermomagnetic effect. The Ettingshausen effect, one such thermomagnetic effect, appears when a transverse magnetic field acts on electric current and produces a temperature gradient in the mutually perpendicular direction. Unlike the Peltier effect, in which the contributions from electrons and holes counteract one another, electrons and holes jointly contribute to the Ettingshausen effect. Consequently, semimetals are ideal candidates for Ettingshausen cooling, and single-crystalline bismuth showed a large ΔT of ~100 K at the hot-side temperature of ~300 K on application of a magnetic field of ~11 T (ref. [30]). Further details on $Bi_{1-x}Sb_x$ for thermoelectric and thermomagnetic cooling can be found elsewhere[13,28].

Bi_2Te_3 alloys. The Peltier effect was initially demonstrated by freezing water droplets into ice at the junction of bismuth and antimony[6]. These semimetals were then used for early measurements of Peltier cooling, with a unicouple consisting of $Bi_{91}Sb_9$ and $Bi_{95}Sn_5$, and showed a small ΔT of only 10 K (ref. [3]). It was not until the 1950s that semiconductors were recognized as promising materials for thermoelectric cooling, with Bi_2Te_3 as the best-in-class candidate. The unicouple of p-type Bi_2Te_3 and n-type Bi was found to exhibit a ΔT_{max} of 26 K at the hot-side temperature of 285 K (ref. [4]). Shortly afterward, the n-type Bi_2Te_3 was produced, and a ΔT_{max} of 40 K was observed for the unicouple of n- and p-type Bi_2Te_3

Box 2 | Thermoelectric cooling modules

Most thermoelectric modules contain a horizontal array of thermoelectric elements: that is, a single-stage module. When several such modules are stacked in a vertical array, a multistage module can be fabricated. Typically, a multistage module is a pyramid shape because the heat dissipated by the upper stage should be removed by the lower stage, and thus more legs are required for the lower stage. The possibility of using such a cascade cooler for augmenting cooling performance was initially proposed by Altenkirch[2] and experimentally confirmed later[6].

The COP of a cascade cooler is[18]

$$COP = \frac{1}{\prod\limits_{n}^{i=1}\left(1 + \frac{1}{COP_i}\right) - 1} \tag{7}$$

where COP_i is the COP of the ith stage, and n is the total number of stages. This reaches a maximum (COP_{max}) when the temperature differences at each stage are chosen so that each stage has an identical COP. The COP_{max} is

$$COP_{max} = \frac{1}{\left(1 + \frac{1}{COP}\right)^n - 1} \tag{8}$$

The temperature difference achievable by a cascade cooler is determined by the separate working temperature intervals at each stage[18]:
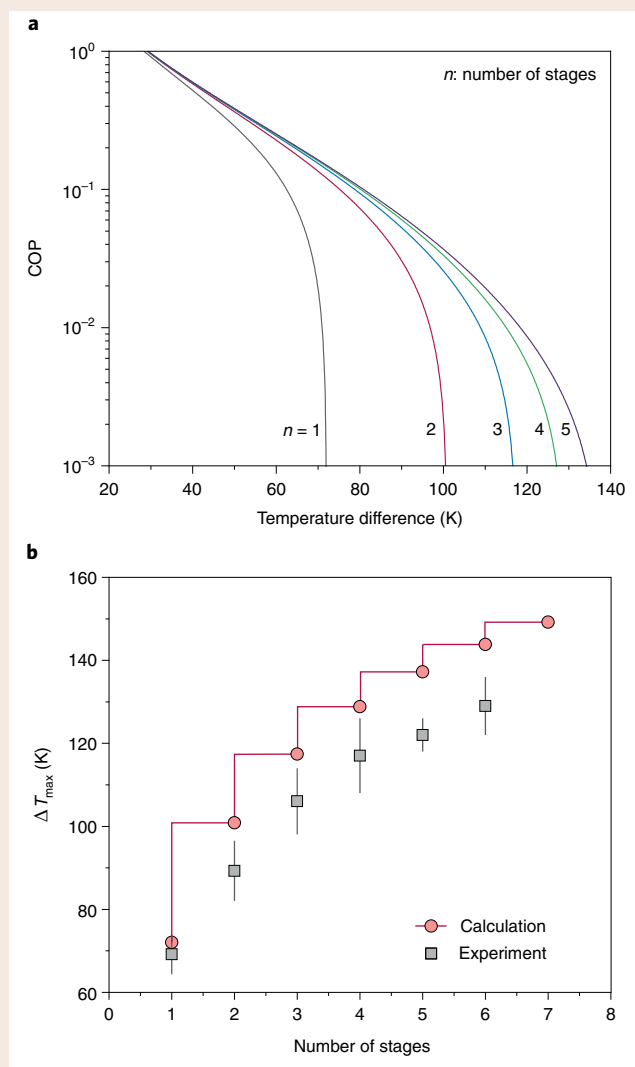
$$\Delta T = \sum_{i=1}^{n} \Delta T_i \tag{9}$$

where ΔT_i is the temperature difference of the ith stage.

When the temperature difference is large, the COP can be effectively improved for multistage modules compared with single-stage modules (part **a** of the figure). Additionally, the ΔT_{max} of a cascade cooler can be notably enhanced with an increasing number of stages, according to Eq. (9). A comparison between the calculated and measured ΔT_{max} for modules with different numbers of stages is shown in part **b** of the figure. A single-stage thermoelectric module can obtain a temperature difference of ~70 K at the hot-side temperature of 300 K. In comparison, a six-stage module can achieve a temperature difference of up to 130 K at the same hot-side temperature[79]. The cooling performance can be further improved by adopting different compositions or materials at each stage — for example, using $Bi_{1-x}Sb_x$ for the upper stage and Bi_2Te_3 alloys for the lower stage. Additionally, it is possible to use optimally graded or segmented legs to augment the thermoelectric cooling performance[80]. However, the cooling capacity of a multistage module is usually limited, so it is primarily used for spot cooling, particularly for detectors, in which the lowered temperature effectively reduces the noise and increases the sensitivity[14].

Comparison of cooling performance between single-stage and multistage modules. a, The calculated temperature-difference-dependent COP for single-stage and multistage modules. **b**, Comparison between calculated and experimental ΔT_{max} (refs. [67,79]) for modules with different numbers of stages. The error bars in the experimental data are obtained by averaging the performance of different commercial thermoelectric modules[67,79]. All of the calculations are based on the temperature-dependent thermoelectric properties of commercial Bi_2Te_3 alloys, and it is assumed that the hot-side temperature is 300 K.

(ref. [31]). Better cooling performance was later reported for zone-melted Bi_2Te_3 and was attributed to its improved homogeneity, adequately controlled impurities and preferred orientation[32]. By this time, the solid-solution alloying strategy for reducing lattice thermal conductivity had just been identified[33]. This was applied to Bi_2Te_3, and improvements in zT were obtained. As a result, ΔT_{max} above 60 K was realized for unicouples of Bi_2Te_3 alloys[5,34].

In the past two decades, improvements in the thermoelectric performance of Bi_2Te_3 alloys have been reported[35]. However, such zT improvements have not yet been engineered into applications, and the performance of commercial coolers has seen little change over this time. At this point, further significant improvement in zT of the Bi_2Te_3 alloys seems to be an ambitious goal. For commercial applications, the large-scale synthesis of Bi_2Te_3 alloys with improved mechanical properties using a cost-effective method with high quality control is as important as zT enhancement. Further details on the development of Bi_2Te_3 alloys for thermoelectric cooling can be found elsewhere[36]. Commercial thermoelectric cooling has been exclusively based on Bi_2Te_3 alloys, with n-type $Bi_2Te_{3-x}Se_x$ exhibiting slightly inferior zT to that of p-type $Bi_{2-x}Sb_xTe_3$. Thus, identifying new n-type materials with high thermoelectric performance is of great importance for potentially replacing the n-type $Bi_2Te_{3-x}Se_x$.
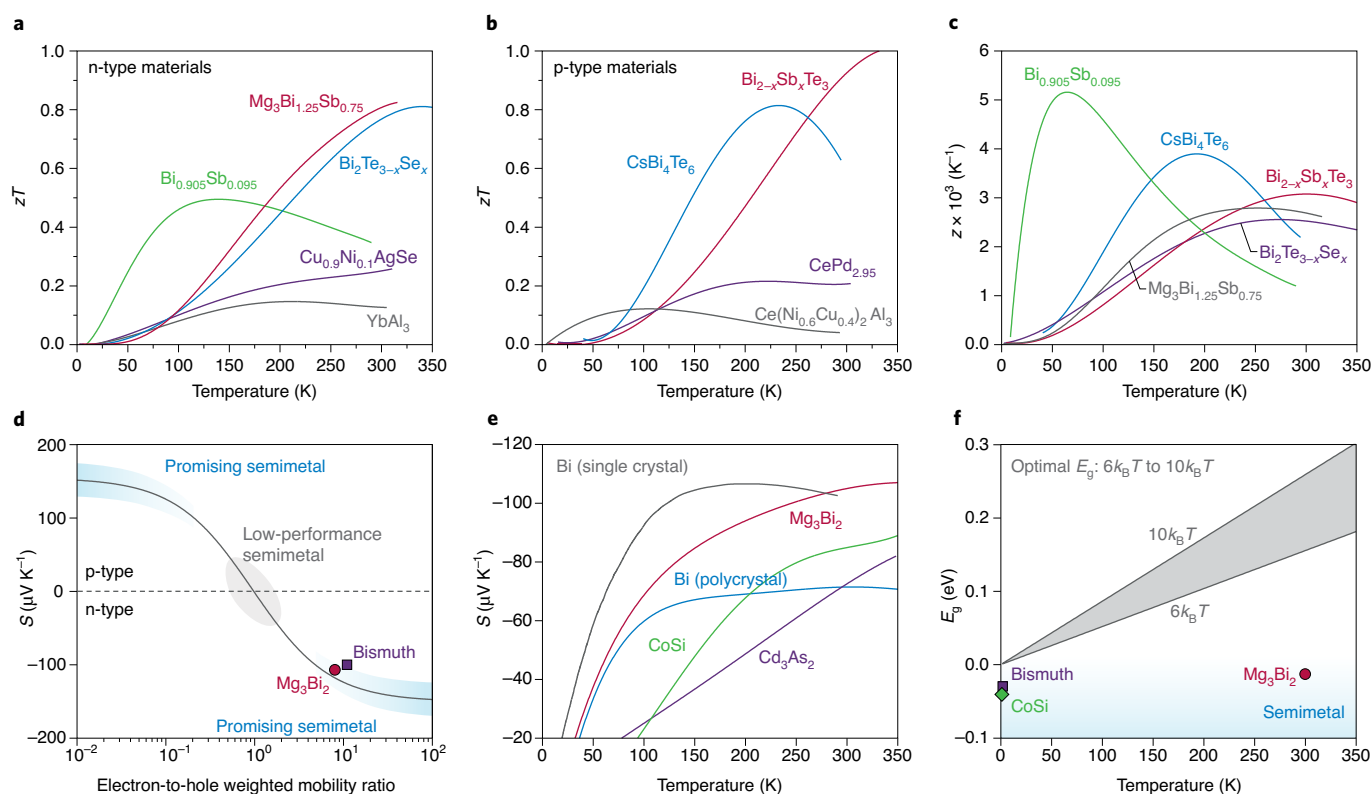
Fig. 2 | Thermoelectric cooling materials. a, b, Summary of the state-of-the-art low-temperature and room-temperature n-type (**a**) and p-type (**b**) thermoelectric materials. The zT of commercial n-type $Bi_2Te_{3-x}Se_x$ and p-type $Bi_{2-x}Sb_xTe_3$ can be found in the Supplementary Information of ref. [22]. **c**, A comparison of the thermoelectric figure of merit z among several high-performance materials. These materials correspond to those in **a** and **b**. **d**, Relationship between the Seebeck coefficient and the electron-to-hole weighted mobility ratio of semimetals. The solid line is calculated by assuming that the band overlap energy is 0.05 eV, the conduction-band density-of-states effective mass is $0.5m_0$ ($0.1m_0$), and the carrier concentration is 2.5×10^{19} cm^{-3} (2×10^{18} cm^{-3}). A very similar solid line can be calculated by using the alternative values in the brackets. **e**, A comparison of the Seebeck coefficient among several semimetals: single-crystalline bismuth (along the trigonal direction)[64], polycrystalline bismuth, polycrystalline Mg_3Bi_2 (ref. [22]), CoSi (ref. [53]) and single-crystalline Cd_3As_2 (ref. [54]). **f**, Relationship between temperature and optimal bandgap energy. Values of band overlap energy for several semimetals — Mg_3Bi_2 (~13 meV)[22], bismuth (~30 meV)[65] and CoSi (~40 meV)[53] — are also shown. The band overlap energy of Mg_3Bi_2 is estimated from the temperature-dependent resistivity, and the corresponding temperature is assumed to be 300 K.

$Mg_3Bi_{2-x}Sb_x$. Compounds based on Mg_3Sb_2 have long been regarded as persistent p-type semiconductors. However, n-type Mg_3Sb_2 was successfully obtained in the 1950s, and the importance of Mg stoichiometry in determining the conduction type was noted[6]. Unfortunately, this result had been overlooked for decades, and n-type Mg_3Sb_2-based materials with high thermoelectric performance were reported only recently[37,38]. Initially, it was the successful conversion from p-type to n-type conduction and the high peak zT in the mid-temperature range[39] that made this compound highly interesting. Subsequently, chemical doping[40] and optimization of processing conditions[41] greatly improved its thermoelectric performance around room temperature, making n-type $Mg_3Bi_{2-x}Sb_x$ comparable to the state-of-the-art n-type $Bi_2Te_{3-x}Se_x$ (ref. [42]). Most recently, further improvements in the average zT of $Mg_3Bi_{2-x}Sb_x$ were reported[43,44]. In contrast to the semiconducting Mg_3Sb_2, Mg_3Bi_2 is a semimetal with a small band overlap energy. Unexpectedly, n-type Mg_3Bi_2 exhibits a high Seebeck coefficient of about −100 μV K^{-1} at ambient temperature (Fig. 2e), which can also be accounted for by its large electron-to-hole weighted mobility ratio (Fig. 2d), similar to bismuth. Tellurium-doped Mg_3Bi_2 showed highly promising electronic properties across a broad temperature range between 150 and 350 K. On further alloying with Mg_3Sb_2, a small bandgap formed, and the lattice thermal conductivity was effectively reduced. As a result, the optimized $Mg_{3.2}Bi_{1.498}Sb_{0.5}Te_{0.002}$ showed a room-temperature zT above 0.7 and a high average zT below

300 K (ref. [22]). A unicouple of n-type $Mg_{3.2}Bi_{1.498}Sb_{0.5}Te_{0.002}$ and p-type $Bi_{0.5}Sb_{1.5}Te_3$ was found to exhibit a ΔT_{max} of ~91 K at a hot-side temperature of 350 K and ~69 K at a hot-side temperature of 300 K. Recently, single-crystalline $Mg_3Bi_{1.25}Sb_{0.75}$ was reported to have an improved average zT (ref. [23]), and a higher cooling performance could be expected. Unlike nanostructured $Bi_2Te_{3-x}Se_x$, which suffers severely from high electrical contact resistance[45], $Mg_3Bi_{2-x}Sb_x$ can be soldered to Cu with a low electrical contact resistance by using Fe or Ni as the metallization layer. Additionally, compared with a zone-melted n-type $Bi_2Te_{2.7}Se_{0.3}$ ingot, which is fragile and thermoelectrically anisotropic, n-type $Mg_3Bi_{2-x}Sb_x$ is mechanically robust[42] and exhibits only weak anisotropy in its thermoelectric properties. The scarcity and high cost of elemental Te could further sway a decision in favour of the low-cost $Mg_3Bi_{2-x}Sb_x$. Recent studies, however, have pointed out the stability issues in using $Mg_3Bi_{2-x}Sb_x$, such as reactivity with moisture and oxygen, and also the ageing effect. Understanding and resolving these problems are vital for promoting n-type $Mg_3Bi_{2-x}Sb_x$ for thermoelectric cooling applications. In addition, large-scale synthesis of n-type $Mg_3Bi_{2-x}Sb_x$ with high quality control is also important for practical application, and thus more effort should be devoted to related research.

Future research in thermoelectric cooling materials
Re-evaluation of existing materials and strategies. Investigating the low-temperature thermoelectric properties of existing

medium- and high-temperature materials would be a meaningful step toward identifying promising cooling materials. Indeed, certain materials that exhibit high zT at medium temperature also demonstrate promising thermoelectric performance below 300 K, examples being PbTe and $Mg_3Bi_{2-x}Sb_x$. It is surprising that the low-temperature thermoelectric properties of many medium- and high-temperature materials have not yet been extensively studied. In addition, since the optimized carrier concentration reduces with decreasing temperature, materials with maximum zT at low temperatures should be less heavily doped[6]. It is essential to minimize contamination by impurities during the synthesis and to reduce the concentration of defects by controlling the composition and preparation conditions.

Additionally, re-evaluation of established strategies that can enhance the zT of medium- and high-temperature materials is essential. As the temperature declines below 300 K, the dominant scattering mechanisms for electrons (acoustic phonon scattering) and phonons (umklapp scattering) can be overshadowed by defect scattering. Thus, it is pivotal to determine whether certain phonon scattering strategies can still improve the ratio of mobility to lattice thermal conductivity at low temperatures. Isoelectronic alloying has proved to be effective in reducing the lattice thermal conductivity and enhancing zT, as is the case in $Bi_{1-x}Sb_x$, Bi_2Te_3 alloys and $Mg_3Bi_{2-x}Sb_x$. However, defects such as dislocations or charged point defects (vacancies and interstitials) can scatter electrons, substantially reducing the carrier mobility at low temperatures. Nanostructures with dimensions in between the electron and phonon mean free paths should scatter more phonons than electrons. However, designing specific nanostructures without introducing additional defects is essential. Currently, the effect of defects on thermoelectric transport properties is not fully understood, so investigating the defect scattering of electrons and phonons is of particular importance[46]. Additionally, band engineering, which is considered an effective approach to improve the power factor, should be re-evaluated. Maximizing the valley degeneracy by converging multiple electronic bands[47,48] (that is, aligning the band edges within the energy difference of $\sim 2k_BT$) becomes more difficult as the temperature decreases. In addition, intervalley scattering, which is often overlooked, could be strong in this case, partially offsetting the benefit of band convergence[49,50].

Exploration of semiconductors with very narrow bandgap. Thermal activation of electrons from the valence band into the conduction band will result in the production of equal numbers of electrons and holes (that is, bipolar conduction) and could greatly reduce zT. To minimize this deleterious effect, a finite bandgap has always been regarded as indispensable for high thermoelectric performance. The optimal bandgap energy (E_g) is predicted to be between $6k_BT$ and $10k_BT$ (refs. [12,51,52]), as shown in the grey shaded area in Fig. 2f. The optimized E_g is in the range 0.16–0.26 eV at 300 K, which explains why narrow-bandgap semiconductors have long been regarded as the most promising candidates for thermoelectric applications. This optimal E_g was predicted by assuming that the electrons and holes have comparable mobilities and density-of-states effective masses — that is, an electron-to-hole weighted mobility ratio of unity. This assumption is not always valid, since the electron-to-hole weighted mobility ratio can be considerably higher or lower than unity. In other words, optimal E_g in the range between $6k_BT$ and $10k_BT$ should not be considered the golden rule, and expanding the exploration to semiconductors with a very small E_g ($<6k_BT$) is also meaningful.

Discovery of promising semimetals. The concept of optimal E_g also implies the exclusion of semimetals (with zero or negative E_g) as promising thermoelectric materials. Admittedly, semimetals are unlikely to exhibit a high zT at medium or high temperatures, owing

to their notable bipolar conduction. Nevertheless, semimetals such as bismuth[27], Mg_3Bi_2 (ref. [22]), CoSi (ref. [53]) and Cd_3As_2 (ref. [54]) exhibit promising thermoelectric properties near room temperature and at low temperatures. The asymmetry in electronic band structures, for example the disparities in the band effective mass and valley degeneracy between the conduction and valence bands, and the accompanying asymmetry in the electron and hole mobilities, as quantified overall by the electron-to-hole weighted mobility ratio, are responsible for their thermoelectric performance. Such asymmetries have been observed in various semiconductors[55] and are expected to exist in many more semimetals[56]. In semiconductors, the effect of the electron-to-hole weighted mobility ratio on the transport properties of semiconductors can be overshadowed by the greatly increased majority carrier concentration through chemical doping. For semimetals, in contrast, owing to the simultaneous presence of the comparable concentration of electrons and holes, the weighted mobility ratio has great importance for the thermoelectric properties. Thus, this parameter can guide the search for promising semimetals. In principle, the weighted mobility ratio could be manipulated if one type of carrier can be preferentially scattered, and thus it is possible to further enhance the zT (ref. [57]).

The band overlap energy is another critical parameter that needs to be taken into account, and it should be small enough (<0.1 eV) to limit the carrier concentration. A lower carrier concentration ($<10^{20}$ cm^{-3}) is essential for a large Seebeck coefficient and a low electronic thermal conductivity. Alloying a semimetal with a semiconductor enables fine-tuning of the band overlap energy or can even open a small bandgap that allows the shifting of the peak performance across a certain temperature range. Such an alloying effect is also beneficial for reducing the lattice thermal conductivity and improving the zT.

Looking ahead to improved materials and systems

Only a small fraction of research effort has been focused on thermoelectric cooling materials in the past two decades, and this partially accounts for the sluggish developments in the field. The slow progress can be easily seen in the dwindling numbers of publications per year on thermoelectric cooling, and it is also evidenced by the difficulty in finding the materials' low-temperature thermoelectric properties among the literature. More focused research effort will be required for future advances.

Bi_2Te_3 alloys have been the state-of-the-art thermoelectric cooling materials for six decades, and commercially available ingots exhibit zT of unity around room temperature. Although improved values of room-temperature zT have been reported for Bi_2Te_3 alloys, the low-temperature properties have often been overlooked, and the cooling performance cannot be assessed. Currently, it is challenging to improve the Bi_2Te_3 alloys further, so discovering promising materials that exhibit higher zT is critical. The recently discovered n-type $Mg_3Bi_{2-x}Sb_x$ represents encouraging progress for such an exploration, but its average zT remains similar to that of commercial n-type $Bi_2Te_{3-x}Se_x$, and further improvement of performance is necessary. As a promising candidate, n-type Ag_2Se with high thermoelectric performance around ambient temperature was reported[58], but its low-temperature properties have been much less studied, and its cooling performance has not yet been characterized. In addition, since the cooling efficiency of a thermoelectric module hinges on both its n-type and its p-type legs, it is also vital to identify high-performance p-type materials. $Bi_{2-x}Sb_xTe_3$ has remained the state-of-the-art p-type material, exhibiting a room-temperature zT superior to that of all other p-type materials. The p-type $CsBi_4Te_6$ is the only material that outperforms $Bi_{2-x}Sb_xTe_3$ below 250 K (ref. [26]) (Fig. 2b), and thus it is a good starting point in the search for new p-type materials. But further studies on $CsBi_4Te_6$ have rarely been reported, and its cooling performance has not yet been evaluated.

Since it is the efficiency of a thermoelectric cooling system that eventually determines its applications, improving the system architecture is of equal importance to the development of materials. Minimizing the thermal resistance and improving the performance of heat-exchanging components are crucial for improving the COP. The relatively high cost of thermoelectric cooling systems also limits wide application[59], so reducing the related expenses is of great economic importance. Thermoelectric materials that are inexpensive and abundant will be favourable, and lowering the cost of heat exchangers and other components is also critical. With concerted progress in materials, devices and systems, both COP improvement and cost reduction are expected and could eventually propel advances in thermoelectric cooling technology.

References

1. Peltier, J. C. Nouvelles expériences sur la caloricité des courants électrique. *Ann. Chim. Phys.* **56**, 371–386 (1834).
2. Altenkirch, E. Elektrothermische Kälteerzeugung und reversible elektrische Heizung. *Phys. Z.* **12**, 920–924 (1911).
3. White, W. Some experiments with Peltier effect. *Electr. Eng.* **70**, 589–591 (1951).
4. Goldsmid, H. J. & Douglas, R. W. The use of semiconductors in thermoelectric refrigeration. *Br. J. Appl. Phys.* **5**, 386–390 (1954).
5. Sinani, S. S. & Gordiakova, G. N. Solid solution $Bi_2Te_3–Bi_2Se_3$ as a material for thermoelements. *Sov. Phys. Tech. Phys.* **1**, 2318–2319 (1956).
6. Ioffe, A. F. *Semiconductor Thermoelements and Thermoelectric Cooling* (Infosearch, 1957).
7. Hempstead, C. & Worthington, W. *Encyclopedia of 20th-century Technology* (Routledge, 2005).
8. Stockholm, J. G. in *CRC Handbook of Thermoelectrics* Ch. 54 (CRC, 1995).
9. Bell, L. E. Cooling, heating, generating power, and recovering waste heat with thermoelectric systems. *Science* **321**, 1457–1461 (2008).
10. Zhao, D. & Tan, G. A review of thermoelectric cooling: materials, modeling and applications. *Appl. Therm. Eng.* **66**, 15–24 (2014).
11. Ziabari, A., Zebarjadi, M., Vashaee, D. & Shakouri, A. Nanoscale solid-state cooling: a review. *Rep. Prog. Phys.* **79**, 095901 (2016).
12. Goldsmid, H. J. *Thermoelectric Refrigeration* (Springer, 1964).
13. Goldsmid, H. J. *Electronic Refrigeration* (Pion, 1986).
14. Stockholm, J. G. Current state of Peltier cooling. In *16th International Conf. Thermoelectrics* 37–46 (IEEE, 1997).
15. Bansal, P. & Martin, A. Comparative study of vapour compression, thermoelectric and absorption refrigerators. *Int. J. Energy Res.* **24**, 93–107 (2000).
16. Riffat, S. B. & Qiu, G. Q. Comparative investigation of thermoelectric air-conditioners versus vapour compression and absorption air-conditioners. *Appl. Therm. Eng.* **24**, 1979–1993 (2004).
17. Gao, M. & Rowe, D. Experimental evaluation of prototype thermoelectric domestic-refrigerators. *Appl. Energy* **83**, 133–152 (2006).
18. Iordanishvili, E. K. & Stilbans, L. S. Thermoelectric microcoolers. *Sov. Phys. Tech. Phys.* **1**, 928–939 (1956).
19. MacDonald, D. K. C., Mooser, E., Pearson, W. B., Templeton, I. M. & Woods, S. B. On the possibility of thermoelectric refrigeration at very low temperatures. *Phil. Mag.* **4**, 433–446 (1959).
20. Mahan, G., Sales, B. & Sharp, J. Thermoelectric materials: new approaches to an old problem. *Phys. Today* **50**, 42–47 (1997).
21. Ishiwata, S. et al. Extremely high electron mobility in a phonon-glass semimetal. *Nat. Mater.* **12**, 512–517 (2013).
22. Mao, J. et al. High thermoelectric cooling performance of n-type Mg_3Bi_2-based materials. *Science* **365**, 495–498 (2019).
23. Pan, Y. et al. $Mg_3(Bi,Sb)_2$ single crystals towards high thermoelectric performance. *Energy Environ. Sci.* **13**, 1717–1724 (2020).
24. Lenoir, B., Cassart, M., Michenaud, J.-P., Scherrer, H. & Scherrer, S. Transport properties of Bi-rich Bi–Sb alloys. *J. Phys. Chem. Solids* **57**, 89–99 (1996).
25. Sun, P., Ikeno, T., Mizushima, T. & Isikawa, Y. Simultaneously optimizing the interdependent thermoelectric parameters in $Ce(Ni_{1-x}Cu_x)_2Al_3$. *Phys. Rev. B* **80**, 193105 (2009).
26. Chung, D. Y. et al. $CsBi_4Te_6$: a high-performance thermoelectric material for low-temperature applications. *Science* **287**, 1024–1027 (2000).
27. Gallo, C. F., Chandrasekhar, B. S. & Sutter, P. H. Transport properties of bismuth single crystals. *J. Appl. Phys.* **34**, 144–152 (1963).
28. Yim, W. & Amith, A. BiSb alloys for magneto-thermoelectric and thermomagnetic cooling. *Solid State Electron.* **15**, 1141–1165 (1972).
29. Wolfe, R. & Smith, G. Effects of a magnetic field on the thermoelectric properties of a bismuth–antimony alloy. *Appl. Phys. Lett.* **1**, 5–7 (1962).
30. Harman, T., Honig, J., Fischler, S., Paladino, A. & Button, M. J. Oriented single-crystal bismuth Nernst–Ettingshausen refrigerators. *Appl. Phys. Lett.* **4**, 77–79 (1964).
31. Goldsmid, H. J. XXVII. Thermoelectric applications of semiconductors. *Int. J. Electron.* **1**, 218–222 (1955).
32. Goldsmid, H. J., Sheard, A. R. & Wright, D. A. The performance of bismuth telluride thermojunctions. *Br. J. Appl. Phys.* **9**, 365–370 (1958).
33. Ioffe, A. F. On thermal conduction in semiconductors. *Il Nuovo Cimento* **3**, 702–715 (1956).
34. Yim, W. M., Fitzke, E. V. & Rosi, F. D. Thermoelectric properties of $Bi_2Te_3–Sb_2Te_3–Sb_2Se_3$ pseudo-ternary alloys in the temperature range 77 to 300 K. *J. Mater. Sci.* **1**, 52–65 (1966).
35. Poudel, B. et al. High-thermoelectric performance of nanostructured bismuth antimony telluride bulk alloys. *Science* **320**, 634–638 (2008).
36. Goldsmid, H. Timeliness in the development of thermoelectric cooling. In *17th International Conf. on Thermoelectrics* 25–28 (IEEE, 1998).
37. Tamaki, H., Sato, H. K. & Kanno, T. Isotropic conduction network and defect chemistry in $Mg_{3+\delta}Sb_2$-based layered Zintl compounds with high thermoelectric performance. *Adv. Mater.* **28**, 10182–10187 (2016).
38. Zhang, J. et al. Discovery of high-performance low-cost n-type Mg_3Sb_2-based thermoelectric materials with multi-valley conduction bands. *Nat. Commun.* **8**, 13901 (2017).
39. Song, S. W. et al. Joint effect of magnesium and yttrium on enhancing thermoelectric properties of n-type Zintl $Mg_{3+\delta}Y_{0.02}Sb_{1.5}Bi_{0.5}$. *Mater. Today Phys.* **8**, 25–33 (2019).
40. Mao, J. et al. Manipulation of ionized impurity scattering for achieving high thermoelectric performance in n-type Mg_3Sb_2-based materials. *Proc. Natl Acad. Sci. USA* **114**, 10548–10553 (2017).
41. Kanno, T. et al. Enhancement of average thermoelectric figure of merit by increasing the grain-size of $Mg_{3.2}Sb_{1.5}Bi_{0.49}Te_{0.01}$. *Appl. Phys. Lett.* **112**, 033903 (2018).
42. Shu, R. et al. $Mg_{3+\delta}Sb_xBi_{2-x}$ family: a promising substitute for the state-of-the-art n-type thermoelectric materials near room temperature. *Adv. Funct. Mater.* **29**, 1807235 (2019).
43. Imasato, K., Kang, S. D. & Snyder, G. J. Exceptional thermoelectric performance in $Mg_3Sb_{0.6}Bi_{1.4}$ for low-grade waste heat recovery. *Energy Environ. Sci.* **12**, 965–971 (2019).
44. Shi, X. et al. Extraordinary n-type Mg_3SbBi thermoelectrics enabled by yttrium doping. *Adv. Mater.* **31**, 1903387 (2019).
45. Liu, W. et al. Understanding of the contact of nanostructured thermoelectric n-type $Bi_2Te_{2.7}Se_{0.3}$ legs for power generation applications. *J. Mater. Chem. A* **1**, 13093–13100 (2013).
46. Liu, Z., Mao, J., Liu, T.-H., Chen, G. & Ren, Z. F. Nano-microstructural control of phonon engineering for thermoelectric energy harvesting. *MRS Bull.* **43**, 181–186 (2018).
47. Pei, Y. Z. et al. Convergence of electronic bands for high performance bulk thermoelectrics. *Nature* **473**, 66–69 (2011).
48. Jeong, C., Kim, R. & Lundstrom, M. S. On the best bandstructure for thermoelectric performance: a Landauer perspective. *J. Appl. Phys.* **111**, 113707 (2012).
49. Norouzzadeh, P. & Vashaee, D. Classification of valleytronics in thermoelectricity. *Sci. Rep.* **6**, 22724 (2016).
50. Witkoske, E., Wang, X., Lundstrom, M., Askarpour, V. & Maassen, J. Thermoelectric band engineering: the role of carrier scattering. *J. Appl. Phys.* **122**, 175102 (2017).
51. Chasmar, R. & Stratton, R. The thermoelectric figure of merit and its relation to thermoelectric generators. *Int. J. Electron.* **7**, 52–72 (1959).
52. Sofo, J. O. & Mahan, G. D. Optimum band gap of a thermoelectric material. *Phys. Rev. B* **49**, 4565–4570 (1994).
53. Fedorov, M. & Zaitsev, V. in *CRC Handbook of Thermoelectrics* Ch. 27, 321–328 (CRC, 1995).
54. Zhang, C. et al. Unexpected low thermal conductivity and large power factor in Dirac semimetal Cd_3As_2. *Chin. Phys. B* **25**, 017202 (2015).
55. Sze, S. M. & Ng, K. K. *Physics of Semiconductor Devices* (Wiley, 2006).
56. Markov, M., Rezaei, S. E., Sadeghi, S. N., Esfarjani, K. & Zebarjadi, M. Thermoelectric properties of semimetals. *Phys. Rev. Mater.* **3**, 095401 (2019).
57. Bahk, J. H. & Shakouri, A. Minority carrier blocking to enhance the thermoelectric figure of merit in narrow-band-gap semiconductors. *Phys. Rev. B* **93**, 165209 (2016).
58. Conn, J. & Taylor, R. Thermoelectric and crystallographic properties of Ag_2Se. *J. Electrochem. Soc.* **107**, 977–982 (1960).
59. LeBlanc, S., Yee, S. K., Scullin, M. L., Dames, C. & Goodson, K. E. Material and manufacturing cost considerations for thermoelectrics. *Renew. Sust. Energy Rev.* **32**, 313–327 (2014).
60. Attey, G. Enhanced thermoelectric refrigeration system COP through low thermal impedance liquid heat transfer system. In *17th International Conf. on Thermoelectrics* 519–524 (IEEE, 1998).

61. Astrain, D., Vián, J. G. & Domínguez, M. Increase of COP in the thermoelectric refrigeration by the optimization of heat dissipation. *Appl. Therm. Eng.* **23**, 2183–2200 (2003).

62. Disawas, S. & Wongwises, S. Experimental investigation on the performance of the refrigeration cycle using a two-phase ejector as an expansion device. *Int. J. Refrig.* **27**, 587–594 (2004).

63. Wang, X., Hwang, Y. & Radermacher, R. Two-stage heat pump system with vapor-injected scroll compressor using R410A as a refrigerant. *Int. J. Refrig.* **32**, 1442–1451 (2009).

64. Issi, J. Low temperature transport properties of the group V semimetals. *Aust. J. Phys.* **32**, 585–628 (1979).

65. Esaki, L. & Stiles, P. BiSb alloy tunnel junctions. *Phys. Rev. Lett.* **16**, 574 (1966).

66. Goldsmid, H. J. in *CRC Handbook of Thermoelectrics* Ch. 48 (CRC, 1995).

67. Raymond, M. & Edward, B. in *CRC Handbook of Thermoelectrics* Ch. 46 (CRC, 1995).

68. Güler, N. F. & Ahiska, R. Design and testing of a microprocessor-controlled portable thermoelectric medical cooling kit. *Appl. Therm. Eng.* **22**, 1271–1276 (2002).

69. Sharp, C. A. III, Doke, M. J., Howarth, R. A. & Recine, L. J. Sr. Compact thermoelectric refrigerator and module. US patent 5,501,076A (1996).

70. Semenyuk, V. in *Thermoelectrics Handbook: Macro to Nano* Ch. 58 (Taylor & Francis, 2006).

71. Hansen, J. & Nussbaum, M. Application of bismuth-telluride thermoelectrics in driving DNA amplification and sequencing reactions. In *15th International Conf. on Thermoelectrics* 256–258 (IEEE, 1996).

72. Lofy, J. & Bell, L. Thermoelectrics for environmental control in automobiles. In *21st International Conf. on Thermoelectrics* 471–476 (IEEE, 2002).

73. Stockholm, J. G. in *CRC Handbook of Thermoelectrics* Ch. 53 (CRC, 1995).

74. Stockholm, J. Prototype thermoelectric air conditioning of a passenger railway coach. In *4th International Conf. on Thermoelectric Energy Conversion* 12 (1982).

75. Sharp, J., Bierschenk, J. & Lyon, H. B. Overview of solid-state thermoelectric refrigerators and possible applications to on-chip thermal management. *Proc. IEEE* **94**, 1602–1612 (2006).

76. Heikes, R. R. & Ure, R. W. *Thermoelectricity: Science and Engineering* (Interscience, 1961).

77. Mahan, G. D. Good thermoelectrics. *Solid State Phys.* **51**, 81–157 (1997).

78. Zebarjadi, M. Electronic cooling using thermoelectric devices. *Appl. Phys. Lett.* **106**, 203506 (2015).

79. Uemura, K.-i. in *CRC Handbook of Thermoelectrics* Ch. 49 (CRC, 1995).

80. Bian, Z., Wang, H., Zhou, Q. & Shakouri, A. Maximum cooling temperature and uniform efficiency criterion for inhomogeneous thermoelectric materials. *Phys. Rev. B* **75**, 245208 (2007).

Acknowledgements

Competing interests

The authors declare no competing interests.

Additional information

Correspondence should be addressed to Z.R.

Peer review information *Nature Materials* thanks Lidong Chen, Ctirad Uher and the other, anonymous, reviewer(s) for their contribution to the peer review of this work.

Reprints and permissions information is available at www.nature.com/reprints.

Publisher's note Springer Nature remains neutral with regard to jurisdictional claims in published maps and institutional affiliations.